J. Physiol. (1973), **235**, *pp.* 333–354
With 12 *text-figures*
Printed in Great Britain

IONIC ANALYSIS OF PHOTORECEPTOR MEMBRANE CURRENTS

BY RALPH ZUCKERMAN

From the Department of Physiology, University of California, School of Medicine, San Francisco, California 94122

(*Received 16 March 1973*)

SUMMARY

1. Membrane current was derived from simultaneous measurements of interstitial 'dark' voltages and conductivities along the radial axis of frog photoreceptor cells. Membrane current was subsequently resolved into its component ionic currents or fluxes by means of ionic substitution and by the use of inhibitors of active transport.

2. The plasma membrane of the frog rod outer segment was found to be permeable to Na^+ and Cl^-, with a ratio of Na^+ to K^+ permeabilities higher than that found in most neuronal cells. A net inward flux of $1{\cdot}5 \times 10^8$ Na^+/sec.rod flows across the outer segment plasma membrane in the dark.

3. The proximal portion of the rod receptor, extending from the proximal region of the inner segment to the synaptic terminal, is mainly permeable to K^+, although some degree of Na^+ permeability is also presumed.

4. A hyperpolarizing electrogenic Na pump was localized to the base of the outer segment and inner segment of the cell. The pump transfers at least 10^8 charges/sec out of the cell at this level, the pump current dividing and re-entering the cell at both the outer segment and proximal portion of the photoreceptor including the synaptic terminal.

5. These findings have been incorporated into an ionic model of the photoreceptor, and its implications for cellular functioning considered.

INTRODUCTION

The vertebrate rod receptor is a structurally differentiated cell capable of signalling the absorption of a single photon in its outer segment to its synaptic terminal some hundred microns away. Recent evidence (Korenbrot, 1972; Zuckerman, 1971, 1972) has suggested that the photoreceptor membrane may be differentiated functionally in terms of its transport mechanisms as well. For this reason, it seemed difficult to describe fully the membrane properties of the photoreceptor segments by means of

intracellular recording. The present report is an attempt to derive the membrane properties of different portions of the cell from an analysis of the potential field around the cell.

The basic approach was first to determine the size and direction of membrane current flowing across radial regions of the frog photoreceptor, and then to break membrane current down into its component ionic currents or fluxes. Treating the retina as an anisotropic and inhomogeneous volume conductor in which current flows to generate a potential field, membrane current (i_m) is related to the potential (V) by a divergence theorem

$$i_m = \nabla \cdot g \nabla V, \tag{1}$$

where ∇ is the vector differential operator and g is the conductivity tensor of the tissue (Rush, 1967; Faber, 1969; Hagins, Penn & Yoshikami, 1970). The radial symmetry of the receptor layer allows the above relationship to be simplified, as the only appreciable voltage gradients which have been observed are in the radial direction. In darkness or with uniform illumination, the frog receptor layer shows tangential (y and z) voltage gradients which are less than 5% of its radial (x) voltage gradient. Eqn. (1), then, can be approximated by

$$i_m \approx \frac{\partial}{\partial x}\left(g_x \frac{\partial V}{\partial x}\right) = \frac{\partial}{\partial x} i_x \tag{2}$$

where i_x is extracellular current flowing in a radial direction, parallel to the long axis of the photoreceptor.

Therefore, the first spatial derivative of radial current may be used to localize regions of photoreceptor membrane which show a net transmembrane current in the dark. The question of which ions carry the current has been investigated by means of ionic substitution and by the use of inhibitors of active transport. These findings have been incorporated into an ionic model of the photoreceptor cell.

METHODS

Frogs (*Rana catesbiana*) were dark adapted for 12–24 hr. The retina was dissected free from the eyecup and pigment epithelium in a pool of oxygenated aspartate Ringer solution under dim red light. The retina was placed receptor-side-up on a piece of no. 50 filter paper. The filter paper was subsequently placed on blotter paper to remove excess fluid and to insure firm attachment of the retina to the filter paper. The filter paper was then placed on a 2·5 × 1·5 cm Lucite plate so that the retina was centered on a 6 mm diameter circle of platinum which served as a current-passing electrode. The Lucite plate was then covered by another piece of Lucite of identical size with a matching 6 mm diameter hole, the region of Lucite around the hole being gradually bevelled to result in a gentle seal around the outer margins of

the retina. Both Lucite plates were covered around the edges by a thin film of silicone stopcock grease and the plates fastened together by small nylon bolts. The lucite insert containing the retina was then placed in a lucite chamber such that the 6 mm diameter circle of retina was aligned with a 6 mm diameter, 5 cm long trough cut in the Lucite block. At the end of this trough was a second circle of platinum which served as the second current-passing electrode. The geometry of the current-passing and recording electrodes is depicted in Fig. 1. An oxygenated stream of Ringer solution filled the trough and perfusion was maintained through the chamber

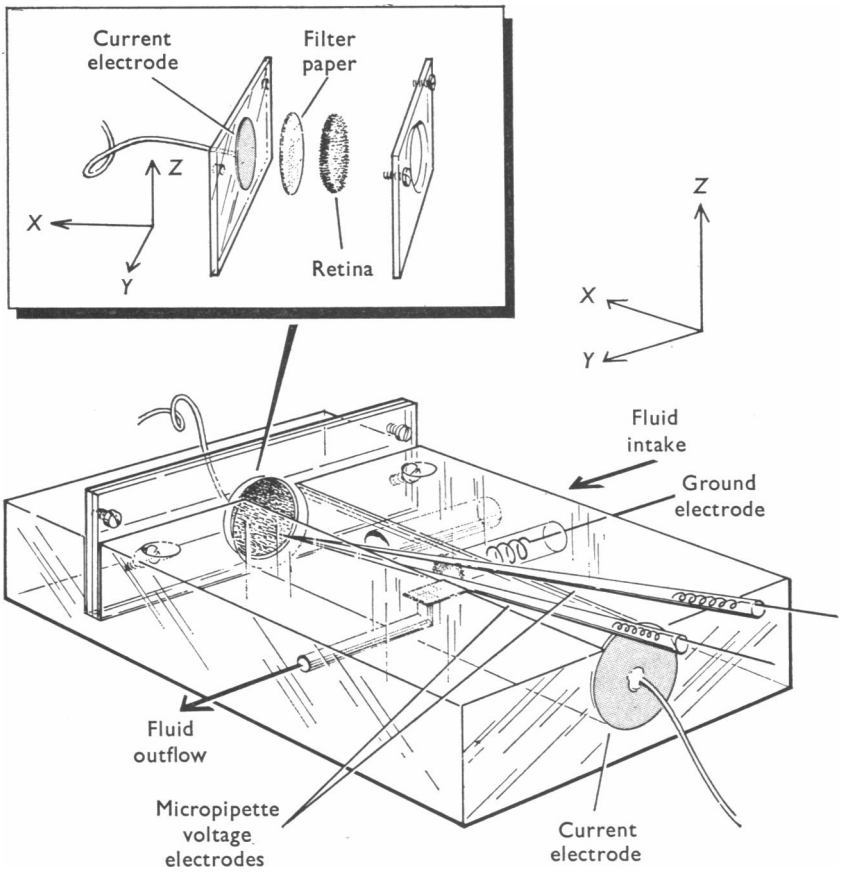

Fig. 1. Schematic view of recording chamber used to measure interstitial resistances and voltages of isolated frog retina. Micropipette electrodes were filled with Ringer solution, solution A, and had tip diameters of 1–2 μm and tip resistances of 5–10 MΩ.

by a gravity feed system with a filter paper drain to reduce turbulence in the perfusate. Perfusion was typically maintained at 2 ml./min. The chamber was also equipped with a suction and syringe system which could rapidly exchange the fluid in the chamber in less than 4 sec. All experiments were carried out at 22° C.

A large Ag·AgCl electrode near the retina grounded the entire chamber. One

micropipette was held in position by a Leitz micromanipulator capable of micron displacement in three planes. The micropipette was brought into contact with the receptor surface of the retina before the chamber was filled with fluid. The criterion for contact was a reduction in the voltage drop to a 10^{-9} A 1 kHz square wave passed through the pipette and connected to ground by a 10 MΩ resistor. The pipette was temporarily referenced to the platinum plate behind the retina. When the pipette tip contacted the retinal surface, the pipette resistance was placed in parallel with the 10 MΩ resistor, thus reducing the amplitude of the 1 kHz square wave. This method allowed accurate determination of the retinal surface as contact with the receptor tips was immediately signalled on the oscilloscope, avoiding delay of the signal caused by amplifier saturation as a result of open circuiting its input. After contact with the receptor surface the pipette was withdrawn 10 μm to insure that it would lie outside the retina at all times. The connexion referencing the pipette to the platinum plate was then disconnected.

A second micropipette, used for penetrating the retina, was held in position by a sealed water-filled hydraulic micromanipulator (Kopf model 607) capable of single micron step advances and withdrawals. The penetrating micropipette was angled approximately 20° with respect to the long axis of the photoreceptors, and pushed into the retina along a plane parallel to the receptor long axes. The linear displacement of the penetrating pipette was transduced into an electrical signal which drove the X-axis of an $X-Y$ plotter. A 1 kHz 10^{-9} A square wave was passed through the penetrating pipette to determine its tip resistance during penetrations and withdrawals. This allowed spurious d.c. potentials caused by tip bending or clogging to be detected. Both micropipettes had tip diameters of 1–2 μm and tip resistances of 5–10 MΩ. The micropipettes were connected by agar salt bridges to Ag·AgCl electrodes mounted in agar saturated with AgCl and shielded from the light.

Each micropipette was connected to a d.c. coupled capacitance-compensated amplifier with unity gain. The amplifiers had input impedances of 10^{13} Ω, input currents of 10^{-13} A, and rise times of 20 μsec with a 10 MΩ compensated electrode. The outputs of the two preamplifiers were fed differentially into a d.c. coupled low-noise, low-drift amplifier (PAR model 113) set for a gain of 100. The output of the secondary amplifier was connected to the oscilloscope, the d.c. coupled Y-axis of an $X-Y$ plotter, and an a.c. coupled 100 Hz chart recorder (Brush Model 220). The low frequency response of the $X-Y$ plotter filtered out the 20 Hz. component of the signal, just displaying the d.c. voltage gradient along the receptor length. Similarly, the chart recorder was a.c. coupled to reject the d.c. component of the signal. Transretinal sine or square-wave currents were injected through the retina by an electrically isolated high-impedance current generator. The current generator had an output impedance of greater than 10^{8} Ω, and was isolated from the recording system by an optical coupler (a photoemissive diode coupled to a photoconductive diode). Leakage from the current generator was less than 0·01 μA/cm² with the diode switched off. Sine wave currents equivalent in amplitude to the flow of 200 μA/cm² of retina or less, at a frequency of 10 or 20 Hz, were typically used.

All solutions were buffered to a physiological pH and showed osmolarities in the physiological range. Sodium aspartate was added in a concentration of 10 mM to all solutions used to perfuse the retina. Measurements with extracellular micropipettes have shown that sodium aspartate isolates light responses of the frog retina to the receptor layer (Sillman, Ito & Tomita, 1969). Moreover, intracellular records from vertebrate photoreceptors (Cervetto & MacNichol, 1972) demonstrate that aspartate interrupts synaptic feedback from the horizontal cell on to the receptor. At the same time, they found no direct effect of aspartate on the resting membrane potential of the receptor in the dark. Consequently, aspartate was used to isolate membrane currents to the receptor cell in the present experiments.

TABLE 1. Solutions

mM	A	B	C	D
NaCl	100	100	0	0
$NaHCO_3$	5	5	1·5	1·5
Na isethionate	0	0	100	100
Na aspartate	10	10	10	10
KCl	3·5	3·5	0	0
$KHCO_3$	0	0	3·5	3·5
$CaCl_2$	0·18	0·18	0	0
Ca aspartate	0	0	0·18	0·18
Glucose	20	20	20	20
Ouabain	0	0·01	0	0·01
m-osmole	236	236	226	226
pH	7·85	7·85	7·85	7·85

RESULTS

Impedance of the retina

In order to convert extracellular voltage gradients into current, it is necessary that the conductivity distribution function of the tissue be known. The d.c. or low frequency impedance of unit volumes of tissue would be expected to be different at different radial depths of the retina, as the high impedance membranes of neurones approach each other to varying degrees and change the extent of extracellular space.

The radial symmetry of the retina insures that voltage gradients generated by the cells lie only in the radial direction. If current injected across the retina can be constrained to flow only in the radial direction as well, then interstitial resistance can be easily determined from the voltage drop to the applied current. The geometry of the chamber and current passing electrodes was designed to do just that, and one simple test for the requirement is shown in the upper portion of Fig. 2. With one micropipette fixed at the receptor surface of the retina, a second micropipette, normally used to penetrate the retina, was pulled back in a radial direction into the fluid just ahead of the tissue. At the same time 10 or 20 Hz sine-wave currents were applied, and the voltage drop measured as a function of pipette displacement. If applied current is flowing in only one direction, then the slope of the sine-wave resistance envelope will be constant. The Figure shows a constant slope proportional to the specific resistance of the Ringer solution. A second test for unidirectional current flow was made by observing the voltage drop measured with two pipettes at the same radial depth in the retina. The voltage drop to applied current with pipettes at the same depth was small compared to that measured by pipettes separated in the radial plane.

The lower portion of Fig. 2 illustrates the inhomogeneous retinal resistance observed upon penetrating the retina during the application of a 20 Hz sine-wave current. The same values for the first spatial derivatives of the wave form envelope were observed irrespective of whether the wave form of the applied current was a square wave or 10 or 20 Hz sine waves. Therefore, the applied current is flowing through the ohmic resistance of the electrolyte in the interstitial spaces rather than through the capacitance of the cell membranes.

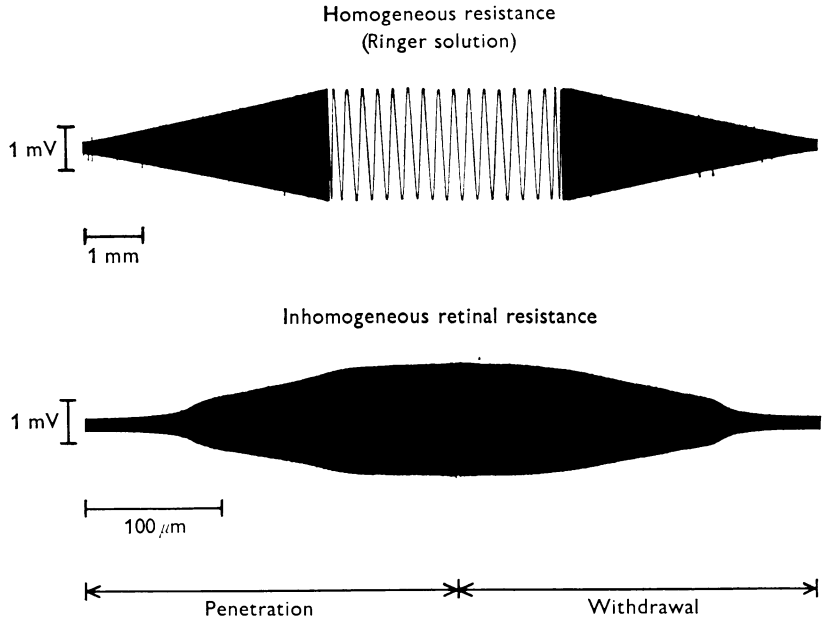

Fig. 2. Upper portion shows test for unidirectional radial current, injected across Ringer solution and retina by an optically isolated constant current sine-wave generator, and measured in Ringer solution ahead of retina. Constant slope of sine-wave resistance envelope indicates unidirectional current flow; see text. Chart recorder speed was increased to show wave form of applied current in centre of Figure. Applied current ~ 125 μA/cm^2 at 20 Hz.

Lower portion shows inhomogeneous retinal resistance measured when pipette penetrated retina during application of 57 μA/cm^2, 20 Hz constant current sine wave. Penetration begins and withdrawal ends with micropipette approximately 30 μm into slowly changing resistance of outer segment layer.

Fig. 3 is a plot of the first spatial derivative of the sine-wave resistance envelope in the region of the photoreceptor layer and slightly beyond. As found by Hagins *et al.* (1970) for rat, interstitial resistance increases rapidly in passing from the region of the frog rod outer segments to the inner segments and outer nuclear layer. A sevenfold increase in interstitial

resistance was observed as the micropipette moved from the distal tip of the rod to its synaptic terminal.

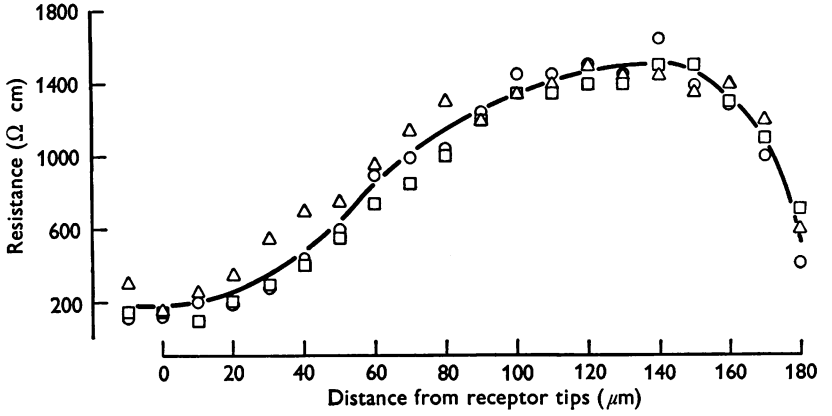

Fig. 3. First spatial differences of sine-wave resistance envelopes for three retinas, taken arbitrarily at 10 μm intervals along the receptor layer and extending into initial portion of inner nuclear layer. Sine-wave voltage excursions induced by applied current ~ 55 μA/cm^2 at 20 Hz.

Transmembrane currents in the dark

Fig. 4 shows typical 'dark' voltage gradients and sine-wave resistance envelopes recorded simultaneously as a micropipette was moved through the receptor layer of the retina. The Ringer-filled micropipette traversed the receptor layer in approximately 10 sec, during which time drift in the micro-electrode system was typically less than 2 μV. Control measurements on retinas treated with 10 mM-KCN or 10^{-5} M ouabain for more than 30 min, showed no detectable d.c. voltage gradients as the pipette moved through the receptor layer. Deformation of the retina by the pipette was occasionally seen in large irregular changes in the slope of the sine-wave resistance envelope. Such spurious changes were usually correlated with large changes in pipette tip resistance, indicative of tip clogging or bending. Spurious data arising from tissue or pipette deformation were thus easily recognized and rejected.

In solution A (see Table 1) the 'dark' voltage increased in the region from 0 to 60 μm; the 'dark' voltage then reversed slope as the pipette moved deeper into the receptor layer, and finally attained a zero slope at the very proximal end of the receptor layer. Such reversals in the 'dark' voltage were observed by Hagins *et al.* (1970) in rat when the retina was maintained in Ringer solution containing a normal complement of physiological buffer with Ca^{2+} and K^+ levels identical to those used in solution A.

Reversal in the 'dark' voltage indicates that there are two oppositely directed loops of 'dark' current flow under the present incubation conditions. One loop flows from somewhere in the middle of the cell distally into the outer segment, while a second loop flows proximally from the same point towards the synaptic end of the photoreceptor. This becomes

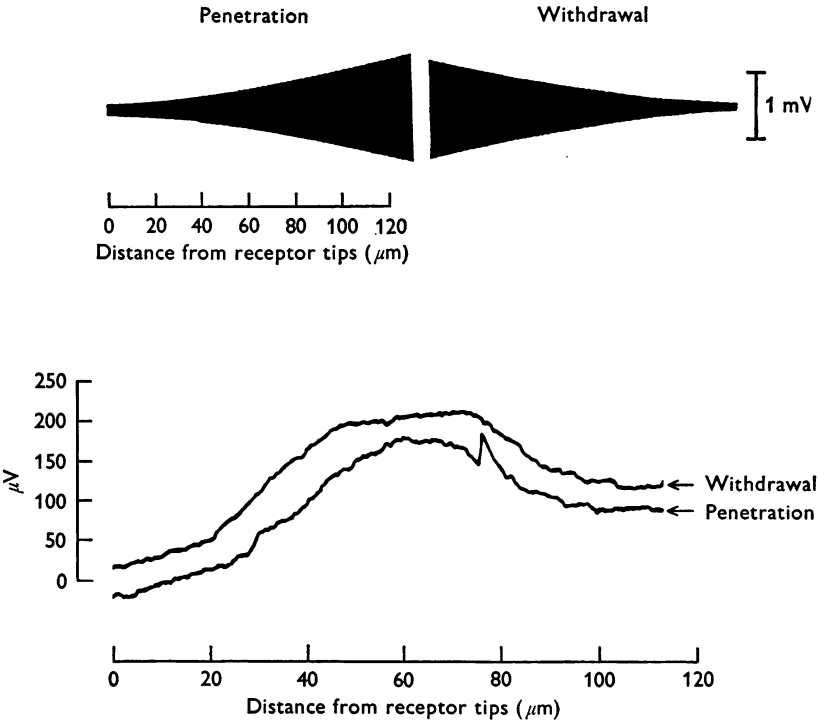

Fig. 4. Simultaneous records of sine-wave resistance envelopes and 'dark' voltage gradients recorded during a cycle of penetration and withdrawal of a pipette along the radial axis of frog photoreceptors. The penetrating pipette traversed receptor layer in approximately 10 sec. Sine-wave voltage excursions induced by applied current ~ 55 μA/cm^2 at 20 Hz. See text.

clearer when the first derivative of voltage is corrected for interstitial resistance to provide values for radial current. Radial current (Fig. 5) is positive (proximal-to-distal current flow) in the region from 0 to 70 μm, then crosses the zero line to reach a peak negative (distal-to-proximal) value at 95 μm and returns to zero at a depth of 120 μm.

The first spatial derivative of radial current is membrane current, which can be most meaningfully expressed in terms of charge transfer per receptor. In order to make the conversion to charge transfer it is necessary that the number of rod receptors per unit area of retina be known. Although

this can be determined from light microscopy of living retinas, the very real possibility exists that receptor density might vary in different portions of the frog retina. Since it is impossible to insure that the micropipette penetrates the tissue in the same portion of each retina, a second approach was sought. Receptor density can be calculated from values of % extracellular space and knowledge of the diameter of a single rod outer segment. Extracellular space can, in turn, be computed from the low frequency impedance along the outer segment region. The method is based upon the well documented assumption that neuronal membranes present an infinite impedance to low frequency current flow (Cole, 1968). In the

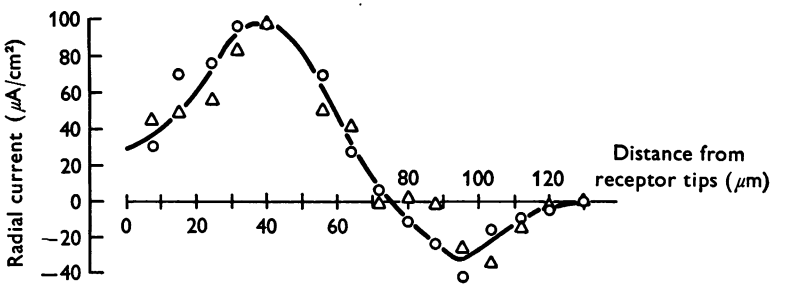

Fig. 5. Radial distribution of 'dark' current. Radial currents calculated from data like Fig. 4 for two retinas in solution A. Radial current was computed by correcting the first spatial derivative of radial 'dark' voltage gradient for interstitial resistance according to Ohm's law.

present experimental chamber, the outer segment layer may be thought of as a cylinder of electrolyte occluded by a parallel array of similarly oriented uniform cylindrical cells. Current in the chamber has been constrained to flow in a direction parallel to the long axes of the outer segments. Therefore, under such conditions, cross-sectional extracellular area or volume will be inversely related to low frequency tissue resistance. Fractional extracellular volume (S), then, will be simply expressed by

$$S = \frac{1}{R}, \tag{3}$$

where R is the ratio of total tissue resistance to extracellular fluid resistance. Tissue resistance along the outer segments was measured along with each determination of the 'dark' voltage gradient, and a mean value of 5·5 μm for the diameter of a single rod outer segment arrived at by viewing outer segments under dim red light. Hence, a single pass of the penetrating pipette through the receptor layer provided sufficient information for the computation of membrane current in terms of charge transfer.

Fig. 6 shows the spatial distribution of transmembrane current in the dark. Current sinks are observed at the outer segment and synaptic ends

of the cell, and a current source in between. More precisely, $1{\cdot}5 \times 10^8$ charges/sec enter the outer segment in the region from 0 to 40 μm; $2{\cdot}1 \times 10^8$ charges/sec leave the junctional region between outer and inner segment, inner segment, rod fibre, and nucleus in the region from 40 to 90 μm; and $0{\cdot}6 \times 10^8$ charges/sec enter the synaptic end of the cell in the

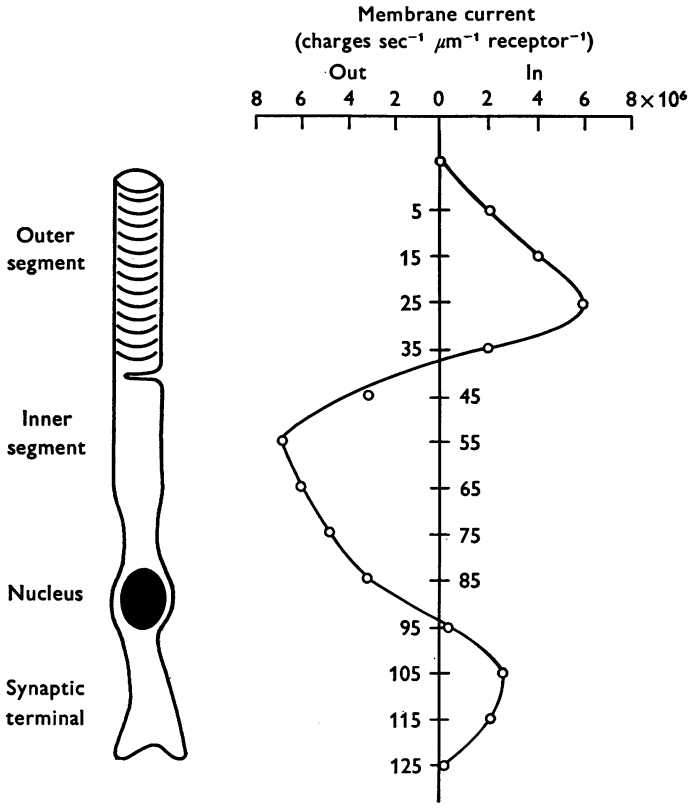

Fig. 6. Radial component of divergence of interstitial current in darkness, expressed in terms of charge transfer per receptor. Data represent first spatial difference of radial 'dark' current calculated from data in Fig. 5. Conversion to charge transfer was made by determination of rod receptor density per unit area of retina during each pass of pipette through receptor layer. See text.

region from 90 to 120 μm. The membrane current distribution in Fig. 6 has been taken as the standard resting or 'dark' distribution of membrane currents for the rod receptor. The ionic analysis which follows applies only to cells which show this distribution of membrane currents.

The sodium pump

The data in Fig. 6 demonstrate that on the order of 10^8–10^9 charges/sec enter each rod in the dark. The only ion suitably distributed across a neuronal membrane to carry this much charge is Na^+. The evidence for the passive influx of Na^+ is considered in the next section, and makes the conclusion quite certain. In any event, the cell needs to transport an equal number of Na^+ out of the cell each second by means of its Na^+ pump in order to maintain intracellular Na^+ at a constant level. The active efflux

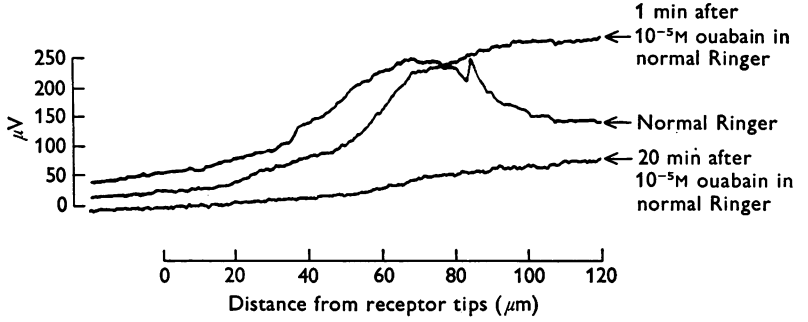

Fig. 7. Typical data of effect of 10^{-5} M ouabain on photoreceptor 'dark' voltages. Pipette traversed receptor layer in approximately 10 sec, during which time drift in micro-electrode system was typically less than 2 μV.

of Na^+ is probably coupled to an active influx of K^+, and the ratio β of Na^+ out/K^+ in determines the electrogenicity of the pump. For a pump which transfers 10^8–10^9 Na^+/sec, even a slight departure of the β value from 1·00 would result in a pump which transfers considerable charge across the membrane, thereby making a direct contribution to membrane current. For this reason, the retina was treated with 10^{-5} M ouabain, and the spatial distribution of membrane current determined.

Fig. 7 illustrates the effect of inhibiting the Na pump on photoreceptor 'dark' voltages. The effect of ouabain is twofold. First, within 1 min of the addition of 10^{-5} M ouabain, the reversal in slope of the 'dark' voltage is permanently abolished. Second, the non-reversing 'dark' voltage subsequently decays with a time constant of 5·5 min and fades out completely in approximately 25 min. Radial current (Fig. 8) after ouabain never crosses the zero line and always remains positive. Therefore, the current loop flowing down to the synaptic terminal is abolished. This immediate effect of ouabain is attributed to suppression of an electrogenic Na pump, as there is little latency between a decrease in pump rate and the observed decrease in pump current. That is, it takes approximately 1 min for ouabain to abolish completely the reversal in the 'dark' voltage shown in

Fig. 7. This is also the approximate diffusion time for ouabain to reach its site of action. For unimpeded diffusion into the retina, it would take about 20 sec for the ouabain concentration to reach $0{\cdot}3 \times 10^{-5}$ M at a depth of 50 μm from the receptor surface, and more than 1 min at 100 μm. Moreover, previous experiments (Zuckerman, 1971) have shown this component of 'dark' current to be profoundly affected by small changes in extracellular K^+ concentration. The slow exponential decrease in the non-reversing 'dark' voltage gradient is attributed simply to ions running downhill along their electrochemical gradients.

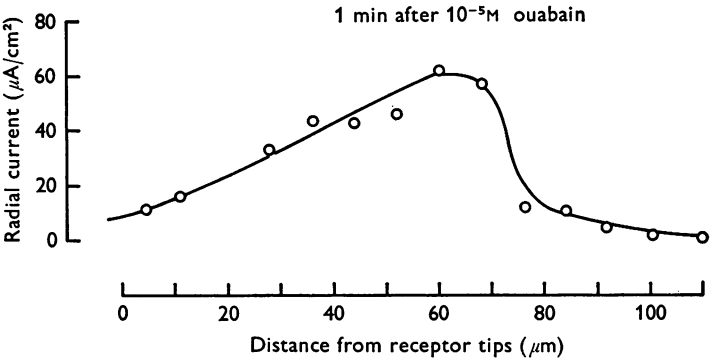

Fig. 8. Radial distribution of 'dark' current 1 min after application of 10^{-5} M ouabain to receptor surface of retina. Radial currents calculated from data like Fig. 7 along with simultaneous records of interstitial resistance.

Considering the immediate effect of ouabain in greater detail, we can compute the spatial distribution of membrane current 1 min after the addition of ouabain. If pumping were electroneutral, $\beta = 1$, then all net fluxes would be passive, and inhibiting the pump should not alter the spatial distribution of membrane current, only decreasing its magnitude as a function of time. Fig. 9 shows that this is definitely not the case. Ouabain causes immediate dramatic changes in the spatial distribution of membrane current. Within 1 min ouabain abolishes outward membrane current along the base of the outer segment, the inner-outer segment junction and inner segment. It reduces inward membrane current along the outer segment; and it abolishes inward membrane current along the synaptic end of the cell, showing a slight reversal to outward membrane current. In frogs, living rods have a length of 50 μm (Korenbrot & Cone, 1972). As shown in Fig. 6, while the pump is operating, the changeover from inward to outward current occurs at a distance of 37 μm from the tips of the rods. In contrast, after suppression of the pump (Fig. 9), the

inward current indicative of a membrane leaky to Na^+ is seen to extend to a distance of 65 μm before dropping off. This establishes the Na^+ pump as a direct source of membrane current localized to the proximal base of the outer segment, the inner-outer segment junction and inner segment regions. The subsequent slow exponential decrease in membrane current is not accompanied by any further significant change in the spatial distribution of transmembrane current. As such, this slow phase can be easily reconciled with the passive movement of ions along their electrochemical gradients after pumping has been abolished.

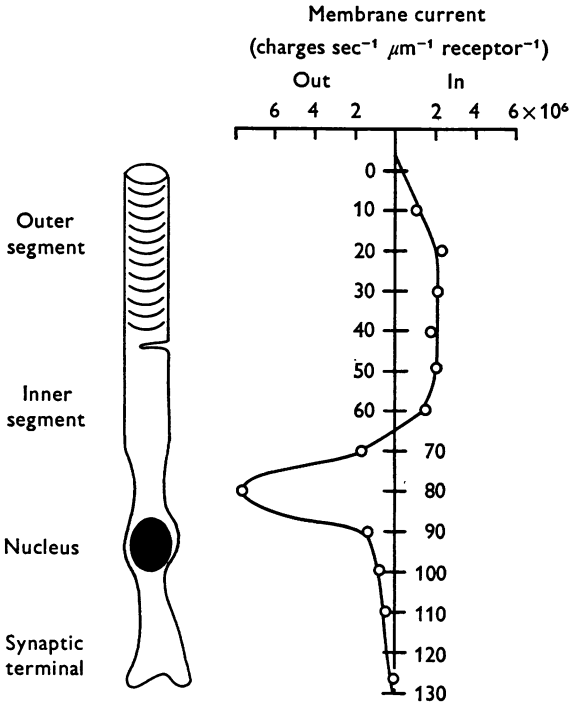

Fig. 9. Radial component of divergence of interstitial current in darkness 1 min after application of 10^{-5} M ouabain, recorded in solution B. Data represent first spatial difference of radial 'dark' current calculated from data in Fig. 8, and expressed in terms of charge transfer per receptor.

Passive ion fluxes

Passive inward charge transfer across the outer segment membrane after ouabain is attributed to an influx of Na^+. A number of lines of evidence support this conclusion. In the present experiments it was impossible to determine the immediate effect of removing $[Na^+]_0$ because of changes in the diffusion potential across the pipette tip as $[Na^+]_0$ equilibrates in the

interstitial spaces, but steady-state effects were observed. In a retina maintained in Na^+-free Ringer for more than 30 min, no detectable 'dark' voltage gradient is observed. In 'dark' voltage gradients measured across the entire retina (Zuckerman, 1971) a rapid electrode reversal technique was used to cancel out diffusion potentials across the electrode tips and the immediate effect of Na^+ removal determined. Replacing $[Na^+]_0$ with $choline^+$ resulted in an immediate (< 4 sec) decrease in proximal-to-distal 'dark' current flow. The present experiments demonstrate that this loop of 'dark' current flows inward across the plasma membrane of the outer segment. Moreover, Korenbrot & Cone (1972) have demonstrated by osmotic experiments on isolated frog outer segments that a passive flux of 10^9 Na^+/sec flows across the outer segment membrane in the dark. Their value for Na^+ influx agrees reasonably well with that measured for inward charge transfer in the present experiments. Taken together, these various lines of evidence strongly support the contention that inward charge transfer across the outer segment membrane is carried by Na^+.

For the outer segment to show appreciable inward charge transfer after ouabain, not only must its plasma membrane be permeable to Na^+, but unlike most other cells, its Na^+ permeability must approach or exceed its K^+ permeability. If this were not the case, then the passive efflux of K^+ after abolishing pumping would oppose the passive influx of Na^+, and little inward charge transfer would be observed. The outer segment, then, is permeable to Na^+, having a ratio of Na^+:K^+ permeabilities higher than that found in most neuronal cells. This conclusion is assured by the observation that ouabain does not alter the passive ion permeabilities of the outer segment membrane (Korenbrot & Cone, 1972).

It remains to determine the anion permeability of the outer segment, as well as the source of outward charge transfer observed along the proximal portion of the photoreceptor after ouabain (Fig. 9). Outward charge transfer after ouabain could be carried by the passive leakage of a cation, K^+, out of the cell, or by the passive leakage of an anion, Cl^-, into the cell. For this reason the experiments were repeated in Cl^--free Ringer in which Cl^- was replaced by the impermeant anion $isethionate^-$ (Fig. 10).

In solution C, Cl^--free Ringer, retinas show the reversal in the 'dark' voltage typically seen in aspartate ringer containing a normal complement of Cl^-. Similarly, the addition of 10^{-5} M ouabain abolishes this reversal in less than 1 min, leaving a non-reversing gradient which decays with an exponential time course. The Figure shows 'dark' voltage gradients recorded within 10 sec of each other both before and after ouabain. The gradients retrace well within 5% of the maximum voltage excursion in both cases.

Fig. 11 compares the passive ion currents observed immediately after

ouabain for normal Ringer and for Cl^--free Ringer. For the comparison, preparations have been selected which show comparable absolute values for interstitial resistance. In this way, the comparison is made between tissues which show similar degrees of electrical shunting around the outer margins of the retina, and differences in the calculated values for transmembrane current must reflect differences in charge transfer across the photoreceptor membranes in the presence and absence of Cl^-.

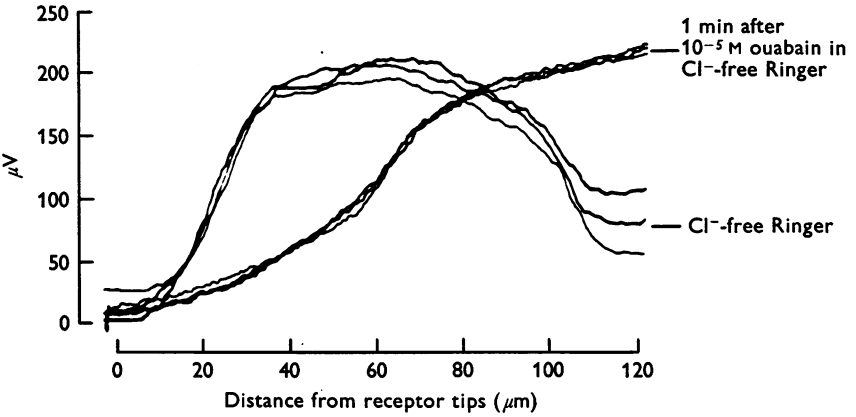

Fig. 10. Dark voltage gradients recorded during three passes of penetrating pipette along receptor layer in Cl^--free Ringer, both before and 1 min after application of 10^{-5} M ouabain. The tracings reproduce within $\pm 5\%$ of maximum voltage excursion in both cases.

Fig. 11 reveals that passive inward charge transfer across the outer segment membrane is considerably increased when Cl^- is removed from the bathing medium around the cells. Inward charge transfer is increased approximately by a factor of two, indicating that a passive influx of Cl^- has been eliminated. The plasma membrane of the outer segment, then, is permeable to Na^+ and Cl^-, with a high Na^+ to K^+ permeability ratio. Outward passive charge transfer along the more proximal parts of the cell is still considerable in Cl^--free Ringer, with but a slight difference between the two conditions. Therefore, outward charge transfer is probably carried mainly by K^+ leaking out of the cell after pumping has been abolished. The portion of the photoreceptor extending from the proximal region of the inner segment to its synaptic terminal is mainly permeable to K^+, although some degree of Na^+ permeability is also presumed.

The fact that passive inward Na^+ flux is greatest near the base of the outer segment in Cl^--free Ringer, and that passive outward K^+ flux is greatest slightly proximal to the inner segment agrees with the localization

of the pump to the base of the outer segment and inner segment. That is, Fig. 9 shows a membrane leaky to Na^+ extending from the tip of the outer segment to the initial portion of the inner segment, and a membrane mainly permeable to K^+ extending from the proximal inner segment to the synaptic terminal. If Na^+ permeability is uniform along the distal portion of the cell, and the K^+ permeability uniform along the proximal portion, then the largest ion gradients to Na^+ and K^+ would exist at the site of the Na^+–K^+ pump. Similarly, after pumping is abolished, the largest inward Na^+ flux would occur at the Na^+ permeable membrane

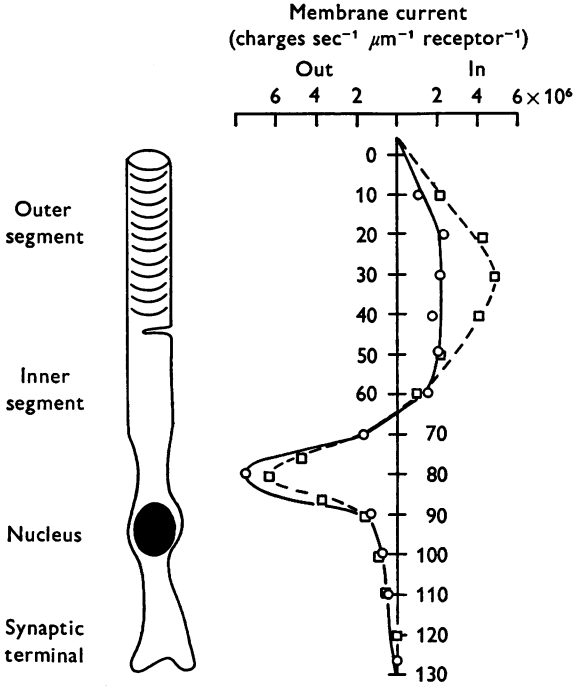

Fig. 11. Comparison of passive transmembrane ion currents recorded in normal Ringer and Cl^--free Ringer, 1 min after application of 10^{-5} M ouabain to receptor surface of retina. Data is expressed in terms of charge transfer per receptor, and represents comparison of preparations which show similar absolute values of radial resistance. Data for Cl^--free Ringer is calculated from data in Fig. 10 along with simultaneous records of interstitial resistance. ○—○, Normal Ringer 1 min after 10^{-5} M ouabain. □– –□, Cl^--free Ringer 1 min after 10^{-5} M ouabain.

nearest the pump, and the largest outward K^+ flux would occur at the K^+ permeable membrane nearest the pump. This would lead to the prediction that the passive influx of Na^+ would be greatest near the base of the outer segment, and the passive efflux of K^+ greatest slightly proximal to the inner segment, so long as pumping is confined to the base of the

outer segment and inner segment regions. Fig. 11 reveals that, in the absence of Cl^- fluxes, the largest Na^+ and K^+ fluxes occur at the predicted regions of the photoreceptor membrane.

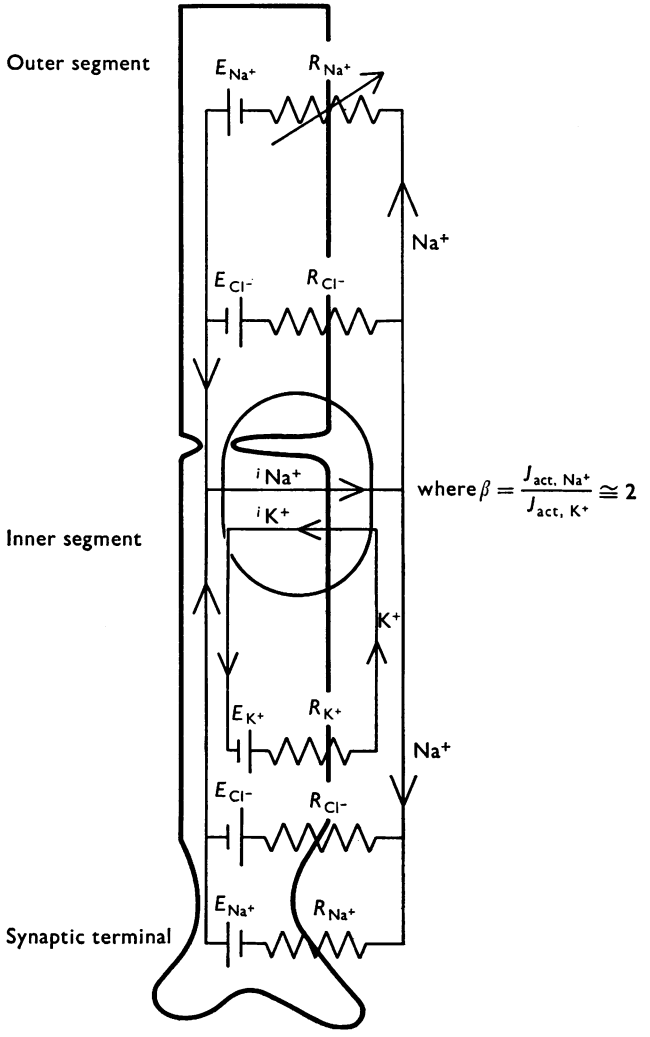

Fig. 12. Proposed ionic model of rod photoreceptor cell. The β value shown for the pump should be considered only a rough approximation. The value is consistent with the measured values for Na^+ influx and the value for charge transferred by the pump.

DISCUSSION

The experimental values taken together allow the following model of the photoreceptor to be constructed. The model relates the membrane properties of the photoreceptor segments to the 'dark' currents observed along the radial axis of the cell. The outer segment is permeable to Na^+ and Cl^-, with a high ratio of $Na^+ : K^+$ permeabilities. This conclusion agrees with the Na^+ and Cl^- permeabilities found by osmotic techniques for isolated outer segments by Korenbrot & Cone (1972), and with their observation that the outer segment is relatively impermeable to K^+ in the dark. Brierley, Fleischman, Hughes, Hunter & McConnell (1968) have similarly shown that outer segment fragments are impermeable to K^+ influx. For this reason, the K^+ battery has been placed in the proximal portion of the cell. The present observations show that the proximal parts of the cell are most permeable to K^+, and a Cl^- limb has been included only for the sake of completeness as Cl^- fluxes across this portion of the cell are minimal. The experiments also suggest some degree of Na^+ permeability for the proximal photoreceptor. However, further experimentation will be necessary to determine whether K^+ and Na^+ permeabilities are uniform along the length of the proximal receptor.

Another key feature of the model is the localization of a hyperpolarizing electrogenic Na^+ pump to the base of the outer segment and inner segment regions. The pump transfers at least 10^8 charges/sec out of the cell at this level. The pump current divides and re-enters the cell at both the outer segment and along the proximal portion of the cell, including the synaptic terminal. At the outer segment, the entering pump current hyperpolarizes the membrane, increasing the driving force on Na^+, reducing the driving force on Cl^-, and thereby increasing inward charge transfer across the outer segment membrane. Similarly, at the synaptic terminal the entering pump current also hyperpolarizes the synaptic membrane, reducing the driving force on an already low level of outward K^+ flux, and considerably increasing the driving force on inward Na^+ movement. This causes a current sink to develop at the synaptic end of the cell. It seems, then, that the component passive and active ion fluxes can be pieced together to reconstruct the basic resting or 'dark' distribution of membrane currents shown in Fig. 6, i.e., current sinks at the outer segment and synaptic ends of the cell and a current source in between.

It has been amply demonstrated that vertebrate photoreceptor membranes hyperpolarize in response to light (Bortoff, 1964; Tomita, 1970; Toyoda, Hashimoto, Anno & Tomita, 1970). The ionic model depicted in Fig. 12 suggests three possible mechanisms by which this could occur (1) a decrease in Na^+ permeability of the outer segment, (2) an increase in

outer segment Cl^- permeability, or (3) an increase in either the rate or electrogenicity of the Na^+ pump. Toyoda, Nosaki & Tomita (1969) measured an increase in the resistance of the receptor membrane to light. This observation is consistent with a light-induced decrease in the Na^+ permeability of the outer segment membrane, although it does not provide conclusive proof. Experiments involving ionic substitution for Na^+ (Sillman *et al.* 1969; Yoshikami & Hagins, 1970; Zuckerman, 1971), as well as osmotic determinations (Korenbrot & Cone, 1972), all support the idea of a light-dependent Na^+ resistance in the plasma membrane of the outer segment. For this reason, a variable resistance has been indicated for the outer segment Na^+ channels in Fig. 12.

Since the primary effect of light is an increase in Na^+ resistance, what then is the functional significance of the electrogenic Na^+ pump? One possible hypothesis is suggested by previous experiments (Zuckerman, 1971, 1972). In these experiments, the effect of light, a reduction in Na^+ influx across the outer segment membrane, was mimicked by a step reduction (1–2 sec) in $[Na^+]_0$, and the response of the electrogenic Na^+ pump determined. The pump responds to a step reduction in Na^+ influx with an exponential decrease in pump current with a time constant of 90 sec. Therefore, during the rapid rising phase of the light response, which occurs in well under 1 sec, the pump serves as a source of constant current. The pump hyperpolarizes the outer segment membrane, driving the membrane potential closer to the Cl^- equilibrium potential and increasing the driving force of inward Na^+ movement. Comparison of peak inward charge transfer in Figs. 6 and 9 reveals that electrogenic pumping increases the peak inward Na^+ 'dark' current at the outer segment by a factor of 3. The presence of electrogenic pumping, then, would also be expected to increase the peak value of the light-induced change in Na^+ current, or photocurrent, by a factor of 3 in response to some given change in Na^+ conductance produced by light. The electrogenic pump, in short, would serve as a boosting mechanism for increasing the photocurrent and photovoltage across the outer segment membrane. The photovoltage across the outer segment membrane would then be conducted decrementally along the length of the photoreceptor membrane to the synaptic terminal, where the release of transmitter substance would be expected to be modulated. The cable losses in signal transmission of the photovoltage from the outer segment to the synaptic terminal would reasonably be expected to be independent of the presence or absence of electrogenic pumping. Consequently, since the presence of a charge-transferring pump would increase the hyperpolarization of the outer segment membrane to light by a factor of 3, the hyperpolarization of the synaptic membrane to light would also be expected to be increased threefold. The boosting effect

of the electrogenic pump on signal transmission could also be phrased alternatively in terms of a simple current-divider analogy. That is, the pump injects constant current out of the middle of the cell, the current re-entering the cell at both the outer segment and proximal portion of the receptor, including the synaptic terminal. When light increases the electrical resistance of the outer segment membrane, it would cause a transient decrease of pump current flowing into the outer segment and a concomitant increase of pump current flowing proximally into the synaptic terminal. The transient increase in current flowing down to the synaptic terminal will hyperpolarize the synaptic membrane to light.

Throughout the discussion it has been assumed that all currents measured in the volume of the receptor layer could be attributed solely to rod membrane currents. However, two additional cell types are found in the receptor layer of frog, viz. cones and Muller cells, and might contribute to the observations. Nilsson (1964) has observed that approximately 35 % of the receptor cells in frog are cones. For the dark adapted retina, the cone cells are recessed from the receptor surface of the retina; i.e., the tip of the cone outer segment appears at the base of the rod outer segment. Consequently, rod outer segments are the only cell type present along the first 40–50 μm of the receptor layer, and the ionic analysis of currents in this region can be attributed solely to rods. Along the inner segment and more proximal region of the rod, both cones and Muller cells are present, and the possibility of contributions from these cells cannot be excluded. Therefore, membrane currents measured in the present work have been simply attributed to the rods, because they are the dominant cell type. Features of the ionic analysis in this proximal region, then, may reflect characteristics of the cone and Muller cell membranes as well. Since the membrane current distributions observed drop off at the synaptic end of the receptor layer, and since the Muller cell continues throughout the more proximal layers of the retina, it is unlikely that Muller cell currents are being observed, unless the Muller cell currents mirror receptor cell activity in the receptor layer of the retina.

A final implication of the model concerns the K^+ permeability of the proximal portion of the photoreceptor, and the consequent possibilities for non-synaptically mediated influences of the photoreceptor on adjacent retinal cells. The receptor membrane hyperpolarizes to light; the hyperpolarization would, in turn, reduce the driving force on K^+ efflux from the cell. A reduced rate of K^+ leakage could reduce $[K^+]_0$ in the interstitial spaces, and thus cause a hyperpolarization of the membranes of adjacent retinal cells which are themselves permeable to K^+. This contention is supported by two observations. First, Cavaggioni, Sorbi & Turini (1972) have observed by tracer techniques that light substantially reduces the

efflux of K^+ from isolated frog retinas. Moreover, the observation of a light-induced K^+ retention was made in retinas perfused with glutamate ions, which limit electrical activity of the retina to the receptor layer. It should be pointed out that aspartate ions were present in all Ringer solutions used for perfusion of the retina in the present experiments. Aspartate like glutamate ions restrict electrical activity to the receptor layer (Sillman *et al.* 1969). Secondly, the data in Fig. 3 demonstrate that interstitial resistance rises sharply in the proximal portion of the receptor layer. This indicates that the volume of the extracellular space is small at this level of the retina, making $[K^+]_0$ particularly susceptible to changes in K^+ leakage from the surrounding photoreceptor cells. The data indicate that extracellular space is as small as 7·0 % of the total tissue volume at the level of the synaptic terminal.

There are two cells in the isolated retina which are likely to be influenced by light-induced changes in $[K^+]_0$. They are the Muller fibres and the horizontal cells. Faber (1969) has observed a light-induced response in the rabbit retina which he has termed 'slow P III', and which shows a distribution of membrane current sources and sinks which associates it with the Muller cell. Slow P III may also be evoked in frog retinas treated with aspartate, and again shows a source and sink distribution which links it to the Muller cell (R. Zuckerman, unpublished). The second cell likely to be influenced by photoreceptor K^+ retention is the horizontal cell. Nelson (1971) has found that horizontal cells in *Necturus* retinas do not show reversal potentials at conventional levels of membrane potential, and has suggested that they are influenced by the ionic milieu which surrounds their synaptic regions.

In the intact eye, the apical processes of the pigment epithelium penetrate into the outer segment layer of the retina, thus reducing extracellular space at this level. Consequently, if the apical membrane of the pigment epithelium is permeable to K^+, it too might be influenced by light-induced changes in $[K^+]_0$. In this regard, it is interesting to note the similarity in the time courses between slow P III and the c-wave of the electroretinogram.

I wish to thank Mr Seymour Winston for expert design and construction of electronic apparatus. I also thank Miss Mary Marti-Volkoff for technical assistance, and Dr Kenneth T. Brown for helpful suggestions. The work was supported by NIH grant EY-00468 to Dr Kenneth T. Brown and by a Fight for Sight grant-in-aid to the author.

REFERENCES

BORTOFF, A. (1964). Localization of slow potential responses in necturus. *Vision Res.* **4**, 627–635.

BRIERLEY, G. P., FLEISCHMAN, D., HUGHES, S. D., HUNTER, G. R. & MCCONNELL, D. G. (1968). On the permeability of isolated bovine retinal outer segment fragments. *Biochim. biophys. Acta* **163**, 117.

CAVAGGIONI, A., SORBI, R. T. & TURINI, S. (1972). Efflux of potassium from the isolated frog retina: a study of the photic effect. *J. Physiol.* **222**, 427–445.

CERVETTO, L. & MACNICHOL, E. F. (1972). Inactivation of horizontal cells in turtle retina by glutamate and aspartate. *Science, N.Y.* **178**, 767–768.

COLE, K. S. (1968). *Membranes, Ions and Impulses.* Berkeley: University of California Press.

FABER, D. (1969). Analysis of the slow transretinal potentials in response to light. Ph.D. Thesis, SUNY at Buffalo, N.Y.

HAGINS, W. A., PENN, R. D. & YOSHIKAMI, S. (1970). Dark current and photocurrent in retinal rods. *Biophys. J.* **10**, 380–412.

KORENBROT, J. I. (1972). Ionic permeabilities of the rod photoreceptor cell. *Biophys. Soc. Abstract*, p. 100*a*.

KORENBROT, J. I. & CONE, R. A. (1972). Dark ionic flux and the effects of light in isolated rod outer segments. *J. gen. Physiol.* **60**, 20–45.

NELSON, R. (1971). Electrical properties of retinal neurons. Ph.D. Thesis, Johns Hopkins University, Baltimore, Md.

NILSSON, S. E. G. (1964). Electron microscopic classification of the retinal receptors of the leopard frog (*Rana pipiens*). *J. Ultrastruct. Res.* **10**, 390–416.

RUSH, S. (1967). A principle for solving a class of anisotropic current flow problems and applications to electrocardiography. *IEEE Trans. biomed. Engng* **14**, 18–22.

SILLMANN, A. J., ITO, H. & TOMITA, T. (1969). Studies on the mass receptor potential of the isolated frog retina. II. On the basis of the ionic mechanism, *Vision Res.* **9**, 1443–1451.

TOMITA, T. (1970). Electrical activity of vertebrate photoreceptors. *Q. Rev. Biophys.* **3**, 179–222.

TOYODA, J. H., HASHIMOTO, H., ANNO, H. & TOMITA, T. (1970). The rod response in frog as studied by intracellular recording. *Vision Res.* **10**, 1093.

TOYODA, J. H., NOSAKI, H. & TOMITA, T. (1969). Light-induced resistance changes in single photoreceptors of necturus and gecko. *Vision Res.* **9**, 453–463.

YOSHIKAMI, S. & HAGINS, W. A. (1970). Ionic basis of dark current and photocurrent of retinal rods. *Biophys. Soc. Abstract*, p. 60*a*.

ZUCKERMAN, R. (1971). Mechanisms of photoreceptor current generation in light and darkness. *Nature, Lond.* **234**, 29–31.

ZUCKERMAN, R. (1972). Photoreceptor dark current: role for an electrogenic sodium pump. *Biophys. Soc. Abstract*, p. 101*a*.